

# **NE 591: Advanced Reactor Materials**

Fall 2021

Dr. Benjamin Beeler

# Last Time

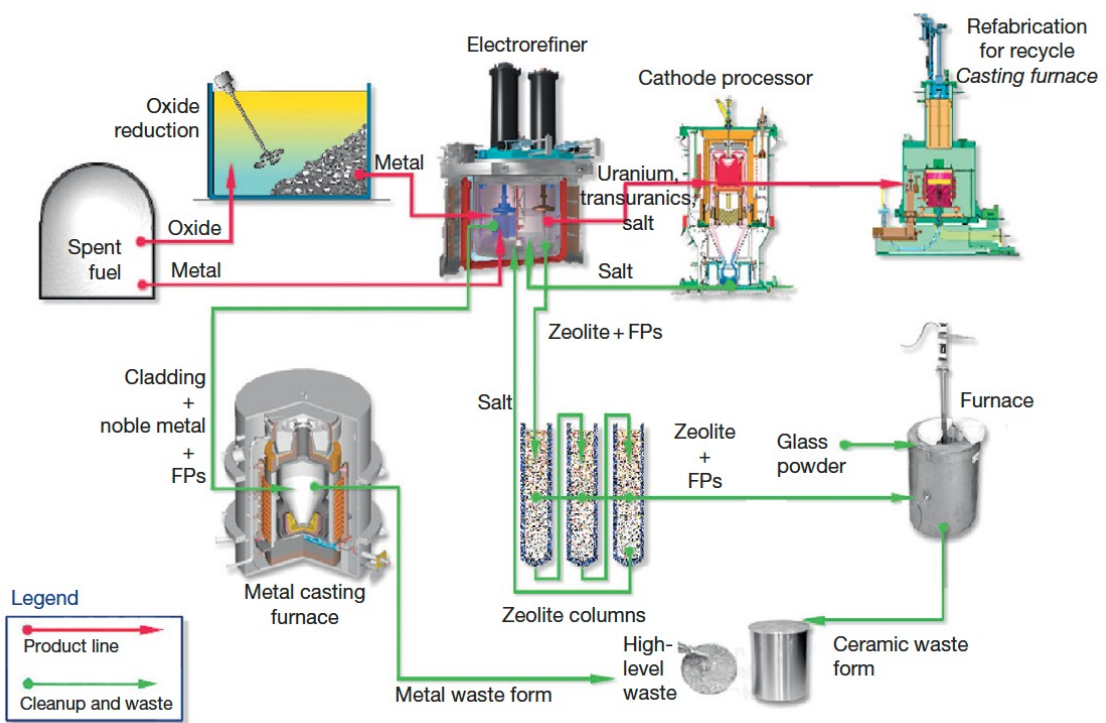
- Completed FCCI for metallic fuels
  - highlighted different compositions, and which species participate
  - Ce and Nd are primary FPs that diffuse into the cladding
  - Fe and Ni diffuse into the fuel
  - melting experiments to test irradiated fuel
- Metal Fuel Fabrication
  - injection casting process

# Reprocessing

- Pyroprocessing
- For more than 50 years, pyrometallurgy has been studied as an alternative strategy in the reprocessing of used fuel
- Pyrochemical processes rely on refining techniques at high temperature (500–900 C) depending on the molten salt eutectic used
- Typically, chloride systems operate at lower temperature compared to fluoride systems, and are preferred in processing
- These processes are mainly based on electrorefining or on extraction from the molten salt phase into liquid metal
- Two processes—one for oxide fuel and one for metallic fuel—have been developed to near industrial scale

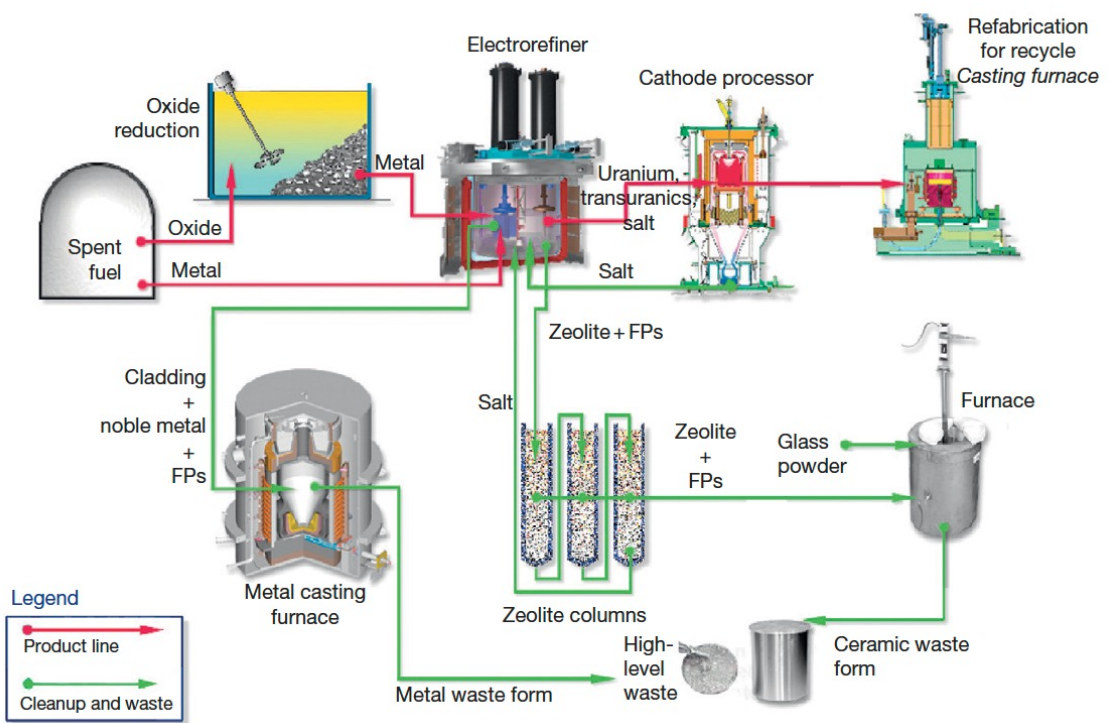
# IFR Pyroprocess

- This process was developed in the US to be part of the IFR project, and can handle the treatment of transuramics
- The fuel is recycled using an electrochemical process based on molten chloride salts and liquid metals
- The molten salt medium for electrorefining is a solution of a certain amount of  $\text{UCl}_3$  dissolved in a  $\text{LiCl}-\text{KCl}$  eutectic



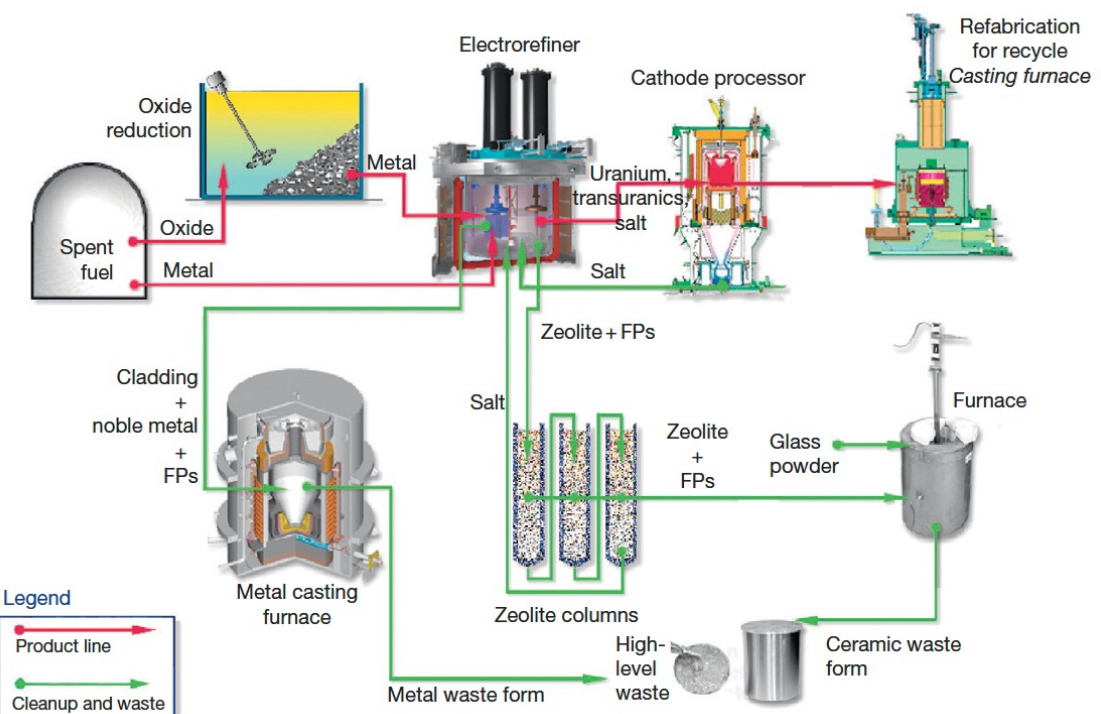
# IFR Pyroprocess

- The fuel is electrochemically dissolved using a potential between the basket (loaded with used fuel) as anode and a stainless steel electrode in the salt as the cathode
- Uranium and TRU are deposited on the anodes
- Once the fuel is dissolved and most of the uranium is deposited on the solid steel, this cathode is replaced by a liquid cadmium cathode, and the remaining TRUs can be codeposited with the remaining uranium



# IFR Pyroprocess

- The alkali, alkaline earth, rare earth, and halide FPs remain primarily dissolved in the salt phase
- More than 90% of the noble metal FPs and fuel alloy material are retained in the chopped fuel cladding segments in the anode baskets
- Can reduce the repository burden of radioactive waste by separating long-lived MA from spent light-water reactor fuel, burning MA in fast reactors, and decreasing the long-term radioactivity of nuclear waste

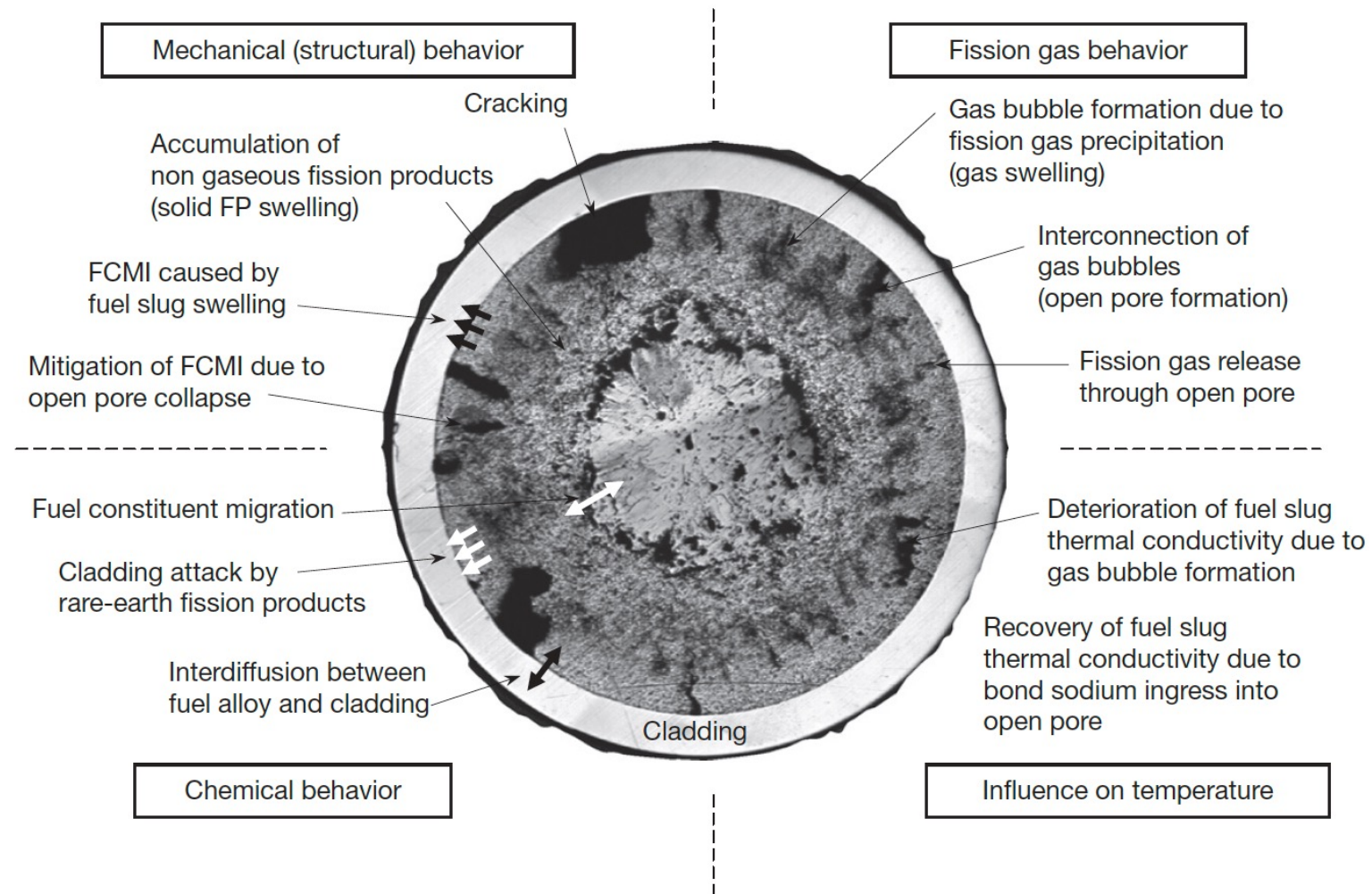


# Refabrication

- Metal-fueled fast reactors facilitate the effective transmutation of MA because of the high-energy neutron spectrum
- One of the measures to load MA into the reactor core is to add MA to the fuel alloy homogeneously
- Can perform injection casting in the same manner as the fresh fuel, to form MA-bearing fuel alloys
- These technologies are expected to reduce the fuel cycle cost even for small-scale fuel cycle plants because of the simplicity of the process and the compactness of the equipment
- For example, in the injection casting process, composition adjustment, melting (alloying), and casting of the fuel slug can be done in a single injection-casting furnace

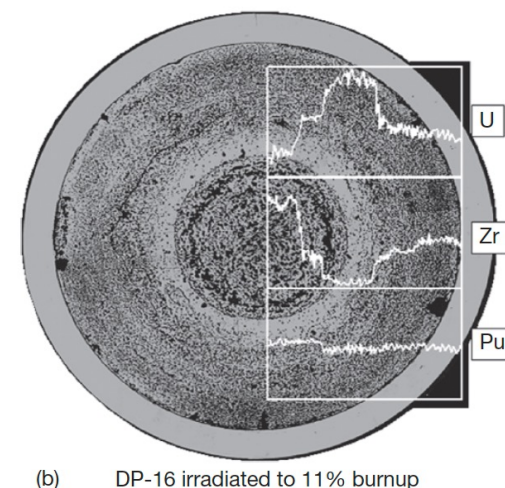
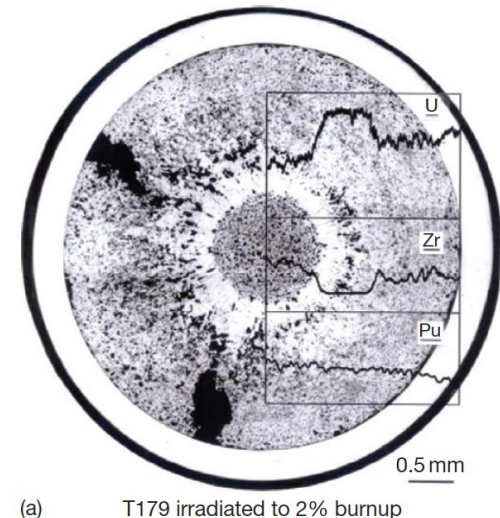
# METALLIC FUEL PERFORMANCE MODELING

# Metallic Fuel Phenomena



# Constituent Redistribution Models

- Constituent redistribution is driven by:
  - temperature gradients in the fuel,
  - solubility gradients in a phase and phase boundaries,
  - additional chemical potentials applied by fuel–cladding gap and cladding
- Results in three concentric zones, namely, a Zr-enriched central zone, a Zr-depleted and U-enriched intermediate zone, and a slightly Zr-enriched zone on the outer periphery
- Migration quickly levels off early in life after a new distribution settles



# Constituent Redistribution Models

- While ternary phase diagrams exist, their accuracy is suspect, and simplified pseudo-binary phase diagrams can be more easily implemented, and removes complexities associated with largely unknown phases
- When applied to a fuel with different Pu content, the phase diagram must be modified accordingly

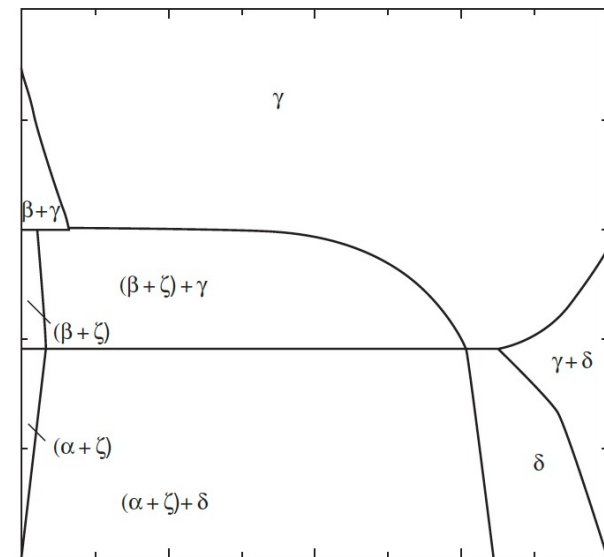
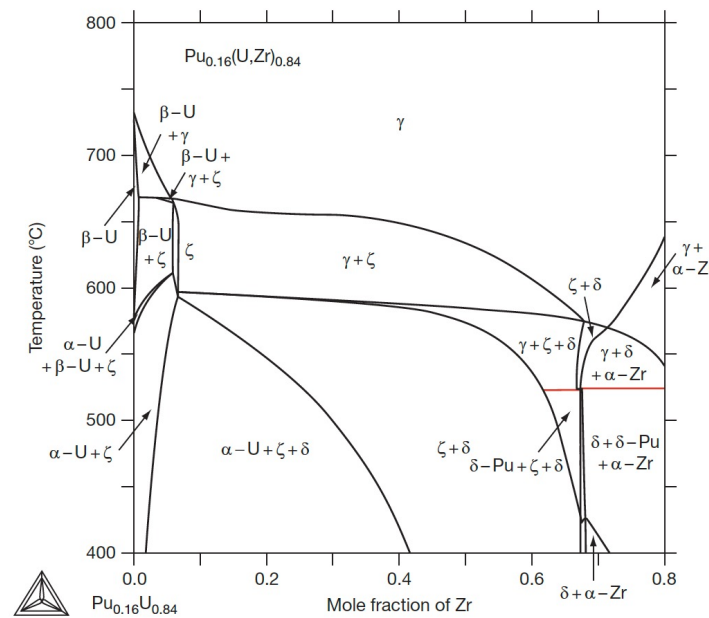


**Figure 6** Simplified pseudo-binary phase diagram of U-19Pu-10Zr.

# Constituent Redistribution Models

- Using the calculated phase fractions, the Fickian and Soret diffusion coefficient are determined
- Artificial factors are used to set the diffusivity in two-phase regions and to scale diffusivities in each phase
- The magnitudes of diffusivities in each phase are largely unknown, and effectively wholly unknown in two-phase regions

BISON Zr Diffusion Model

$$\begin{aligned} D(x, T) &= D_\pi(x, T) \\ S(x, T) &= D_\pi(x, T) \left( \frac{x(1 - x_{\text{Pu}} - x)}{1 - x_{\text{Pu}}} \right) \frac{Q_\pi^*}{RT^2} \\ S(x, T) &= f_\beta D_\beta(X_\beta(T), T) \left( \frac{X_\beta(T)(1 - x_{\text{Pu}} - X_\beta(T))}{1 - x_{\text{Pu}}} \right) \left( \frac{\Delta H_\beta + Q_\beta^*}{RT^2} \right) \\ &\quad + (1 - f_\beta) D_\gamma(X_\gamma(T), T) \left( \frac{X_\gamma(T)(1 - x_{\text{Pu}} - X_\gamma(T))}{1 - x_{\text{Pu}}} \right) \left( \frac{\Delta H_\gamma + Q_\gamma^*}{RT^2} \right) \end{aligned}$$

# Temperature Predictions

- Constituent redistribution relies on accurate temperature profiles
- Fuel temperature is affected by the thermal conductivity of the fuel, which in turn is changed by porosity evolution and sodium infiltration, in addition to changes in Zr concentration
- BISON thermal conductivity models exist for the distinct phases/species, and account for degradation of thermal conductivity

$$\begin{aligned} k_U &= 21.76 + 1.665 \times 10^{-2}T + 5.167 \times 10^{-6}T^2, \\ k_{Pu} &= -8.162 + 4.841 \times 10^{-2}T - 1.614 \times 10^{-5}T^2, \\ k_{c,U-Zr} &= -97.0 + 177.9f_{Zr} - 95.94f_{Zr}^2 + 8.351 \times 10^{-3}T \\ &\quad + 2.931 \times 10^{-5}T^2 - 5.694 \times 10^{-3}f_{Zr}T \\ k_{c,Pu} &= -135.8 - 29.89w_{Pu} + 351.9w_{Pu}^2 + 0.3571 - 1.186 \times 10^{-4}T^2 - 0.961w_{Pu}T \end{aligned}$$

$$k = f_p k_o$$

$$f_p = \frac{1-p}{1+\beta_p p}$$

$$f_{p-Na} = \left[ 1 - 3 \cdot \frac{1 - k_{Na}/k_f}{2/\varepsilon + (3 - 2/\varepsilon)(k_{Na}/k_f)} \cdot \frac{p_{Na}}{1-p_g} \right]$$

# Porosity Predictions

- BISON utilizes a simplified model for porosity
- The mechanical force balance on an equilibrium bubble can be expressed by the Young-Laplace equation
- Making assumptions for creep stress, bubble size, can calculate swelling due to fission gas
- Finally, can determine porosity from the swelling
- Solid fission products are a function of fission density

$$p = \frac{2\gamma}{r_b} - \sigma_h + \sigma_{cr}$$

$$pV = vRT$$

$$V = \frac{vRT}{\frac{2\gamma}{r_b} - \sigma_h + \sigma_{cr}}.$$

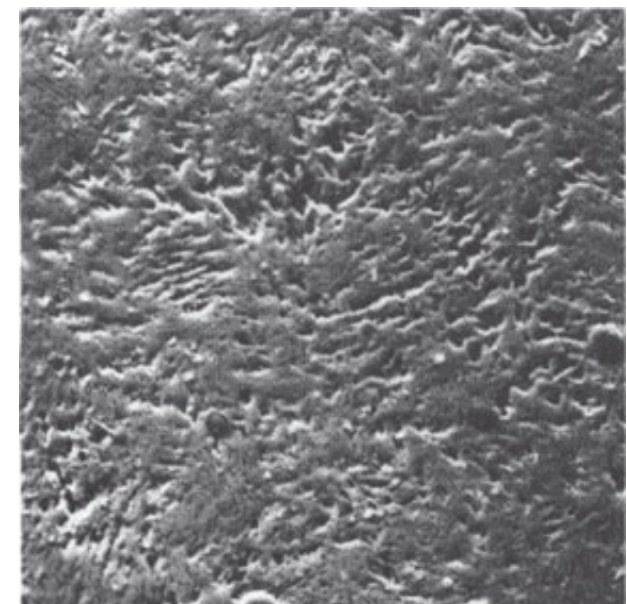
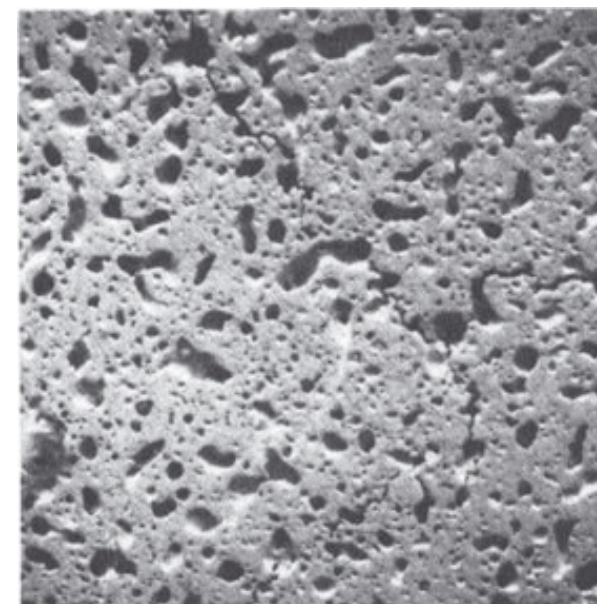
$$\left(\frac{\Delta V}{V_0}\right)_g = \frac{3.59 \times 10^{-24}FT}{1.01 \times 10^7 - \sigma_h}$$

$$p = \frac{\left(\frac{\Delta V}{V_0}\right)_g}{\left(\frac{\Delta V}{V_0}\right)_g + 1}$$

$$\left(\frac{\Delta V}{V_0}\right)_s = 4.16 \times 10^{-29}F$$

# Porosity Predictions

- These porosity models don't incorporate different phases, initial porosity, axial/radial swelling, etc.
- These models have been updated slightly to improve code robustness, but still don't incorporate these critical microstructural phenomena



# Mechanical Properties

- Young's Modulus

$$E = E_u(1 - \beta_E P) \left( \frac{1 + 0.17W_{Zr}}{1 + 1.34W_{Zr}} - W_{Pu} \right) \left( 1 - 1.06 \left[ \frac{T - 588}{T_{mu}} \right] \right)$$

- Poisson's ratio

$$\nu = \nu_u(1 - \beta_p P) \left( \frac{1 + 3.4W_{Zr}}{1 + 1.9W_{Zr}} \right) \left( 1 + 1.2 \left[ \frac{T - 588}{T_{mu}} \right] \right)$$

- Creep

$$\dot{\epsilon} = A_4 (1 - p^{0.67})^{-3} \exp\left(\frac{-Q_3}{RT}\right) \sigma^3 + A_3 F \sigma$$

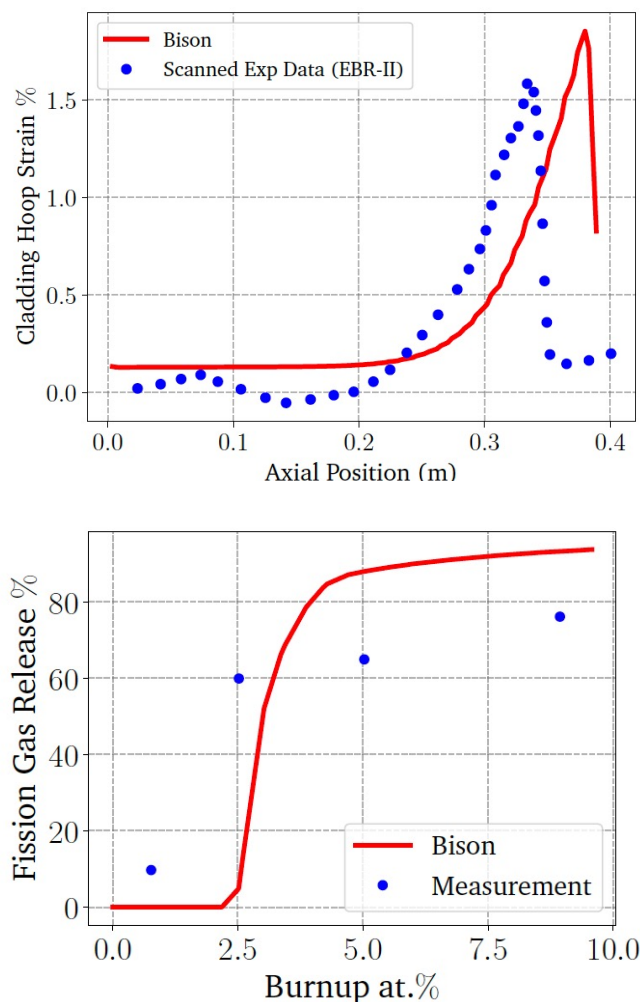
- Cladding models for HT-9 creep and  $k_{th}$

$$\dot{\epsilon}_{cr} = C_5 \exp(-\frac{Q_4}{RT}) \bar{\sigma}^2 + C_6 \exp(-\frac{Q_5}{RT}) \bar{\sigma}^5 + [B + A \exp(-\frac{Q}{RT})] \phi \bar{\sigma}^{1.3}$$

$$k = 17.622 + 2.42 \times 10^{-2}T - 1.696 \times 10^{-5}T^2, \quad T < 1030 \text{ K}$$

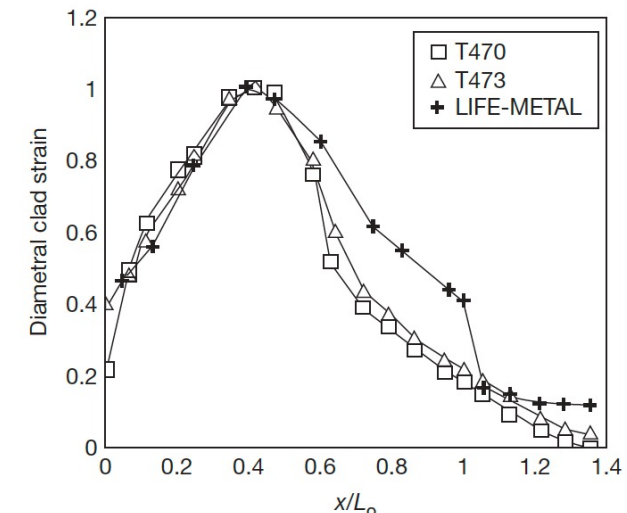
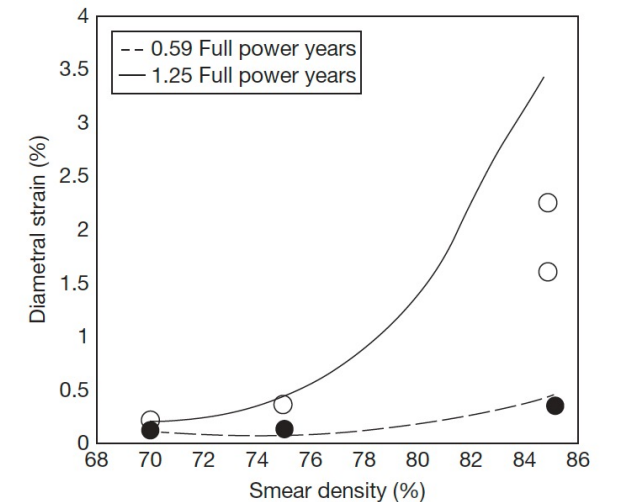
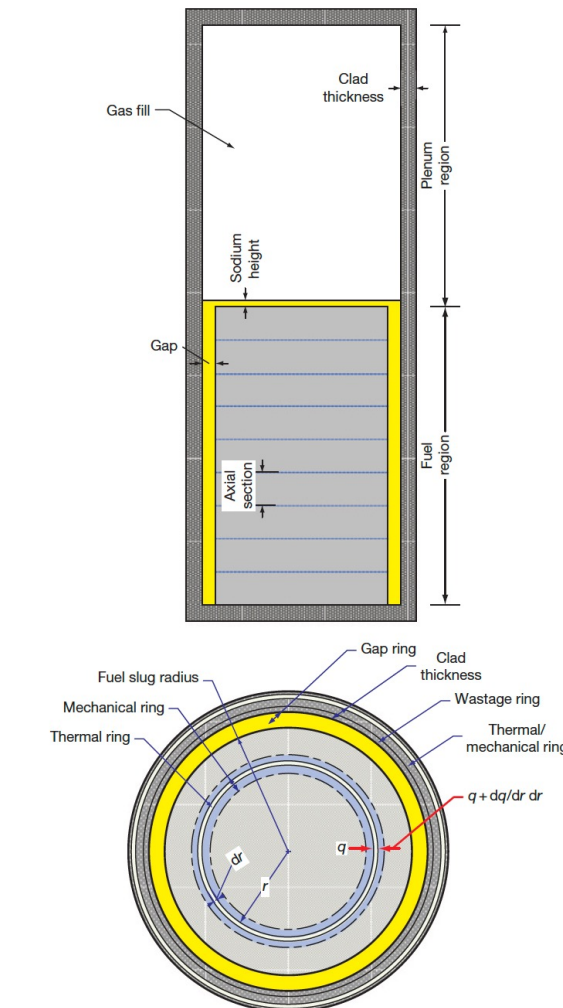
# BISON Testing

- BISON can handle binary and ternary fuel and compare reasonably well with EBR-II data
- Discrepancies are due to inadequate knowledge of materials models, and underlying issues with material descriptions, and code robustness
- Development is ongoing, and improvements to swelling models, for example, have been made



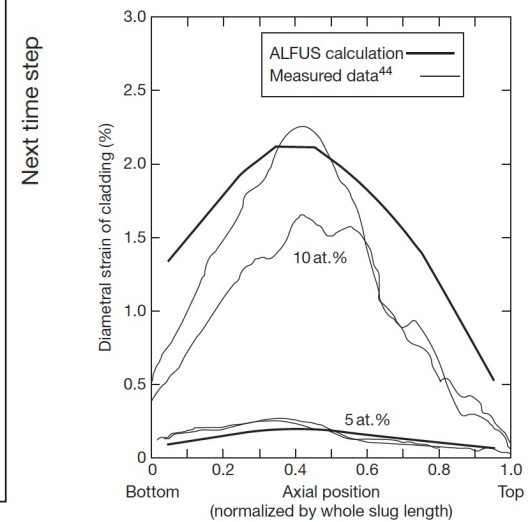
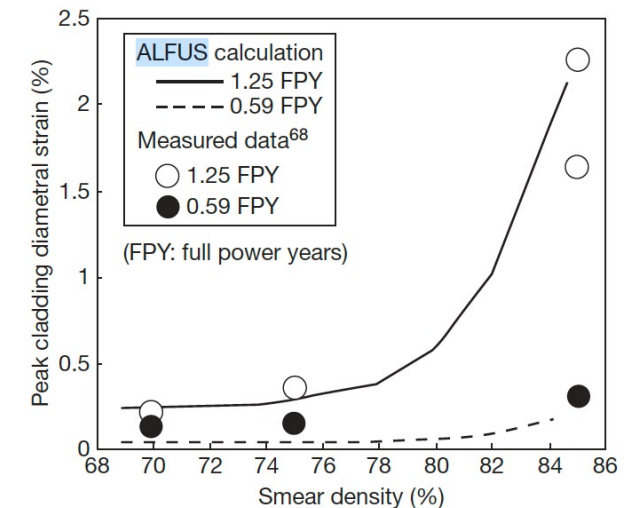
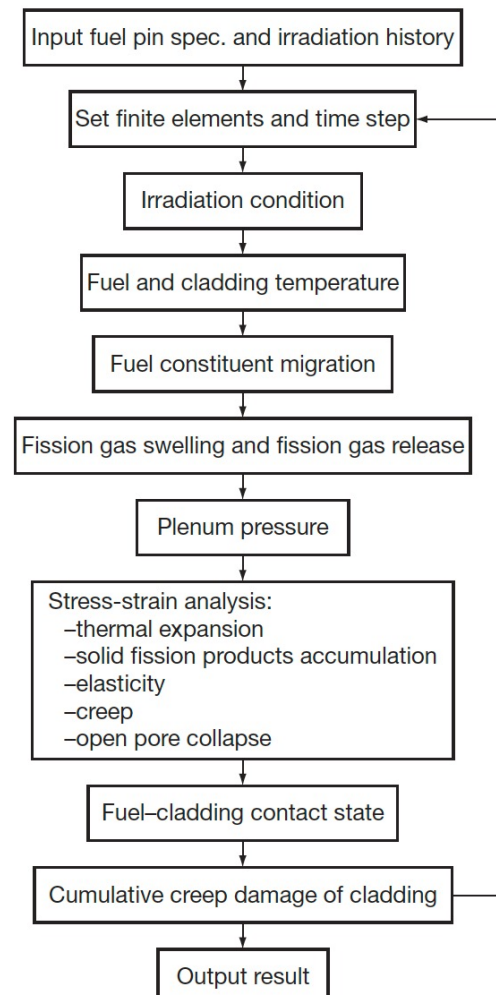
# Other Codes

- LIFEMETAL
- The code has evolved from the LIFE series of codes from ANL that perform steady-state and transient analyses for nuclear fuel
- The original code was developed for UO<sub>2</sub> and mixed oxide fuels for use in fast reactor systems
- The code was developed in association with the IFR and has been extensively used for planning steady state and transient experiments at EBR-II



# Other Codes

- ALFUS
- JAEA code that is multiphysics in nature and focuses on the mechanical behavior of the fuel under irradiation
- Both LIFE-METAL and ALFUS are capable of simulating metal fuel irradiation behavior to some extent
- Both lack different swelling in different radial zone, coupling of redistribution, realistic predictions of FCCI



# MIXED OXIDE FUEL

# MOX Introduction

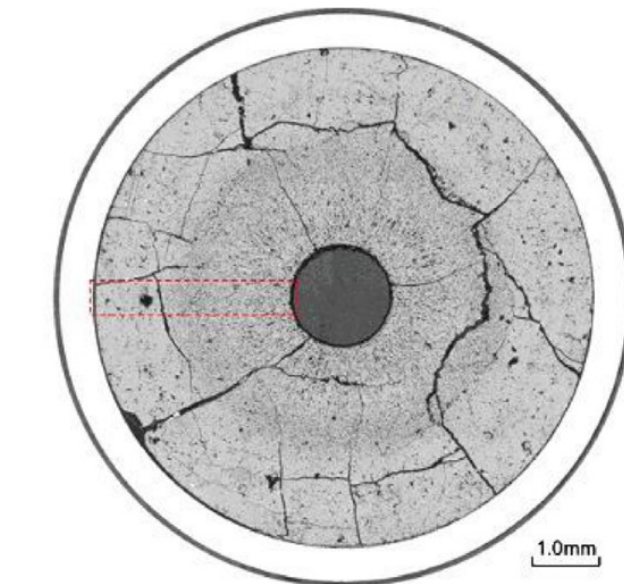
- Despite some disadvantages, such as its low U density, poor thermal conductivity, and its chemical reaction with sodium, MOX fuel ( $\text{U},\text{Pu}\text{O}_2$ ) is the fuel that has been used most in fast reactors
- In order to avoid the dramatic swelling of metallic fuels, MOX fuels were explored in fast reactors
- Behavior was observed to be satisfactory and was relatively widely implemented in SFRs

**Table 1** Main characteristics of standard fuel pins irradiated in the prototype and commercial fast reactors ( $\rho > 200 \text{ MWth}$ )

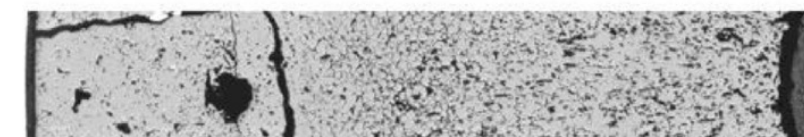
	BN350	Phénix	PFR	BN600	FFTF <sup>a</sup>	Super-Phénix	MONJU
First criticality	1972	1973	1974	1979	1980	1985	1994
Thermal power (MWth)	750	563	600	1470	400	3000	714
Electric power (MWe)	350 <sup>b</sup>	250	250	600	—	1200	280
Type of fuel	$\text{UO}_2$	$(\text{U},\text{Pu})\text{O}_2$	$(\text{U},\text{Pu})\text{O}_2$	$\text{UO}_2$	$(\text{U},\text{Pu})\text{O}_2$	$(\text{U},\text{Pu})\text{O}_2$	$(\text{U},\text{Pu})\text{O}_2$
No. of subassemblies (inner/outer core)	109/117	55/48	28/44	209/160	28/45	193/171	108/90
No. of pins per assembly	127	217	325	127	217	271	169
Type of spacer	Wire	Wire	Grids	Wire	Wire	Wire	Wire
Length of pin (m)	1.8	1.793	2.25	2.445	2.38	2.7	2.813
Height of fissile column (m)	1.06	0.85	0.914	1.0	0.914	1.0	0.93
Lower fertile column length (m)	0.4	0.3	0.45	0.4	—	0.3	0.35
Upper fertile column length (m)	0.57	0.31	0.45	0.4	—	0.3	0.3
Clad outer diameter (mm)	6.9	6.55	5.8	6.9	5.84	8.5	6.5
Clad thickness (mm)	0.4	0.45	0.38	0.4	0.38	0.565	0.47
Helical wire diameter (mm)		1.15			1.42	1.2	1.32
Pellet diameter (mm)		5.42				7.14	5.4
Fuel clad diametral gap (mm)		0.23			0.14	0.23	0.16
Central hole diameter (mm)	0	0	1.5	0		2.0	0
Fissile atoms/(U + Pu) (%) (inner core/outer core)	17/26	18/23	22/28	17/26	20/25	15/22	16/21
Fuel density (% TD)	95	95.5	97	95	91	95.5	85
Smeared density (%)	75	88	78	77	86	83	80
Plenum volume (cm <sup>3</sup> )	8	13	14	21	19	43	28
Maximum linear power (W cm <sup>-1</sup> )	400	450	420	472	413	470	360
Peak cladding temperature (°C)	570	650	670	700	660	620	675
Maximum neutron flux ( $10^{15} \text{ n cm}^{-2} \text{ s}^{-1}$ )	7	7.1	7.6	7.7	7	6	6.0
Maximum burnup (at.%) (GWd t <sup>-1</sup> )	9.0	16.9	23.5	11.8	24.5	Not relevant	Not relevant
Maximum dose (dpa)	60	156	155	90	—	—	—

# MOX Fuels in SFRs

- SRFs with MOX fuel will lead the MOX to run at higher temperatures than LWR fuel, and thus with different properties
- Fission product phases and evolving microstructures create highly localized properties that can differ significantly from the bulk fuel
- Stoichiometry and Pu content are important factors that dictate thermal properties



(a)



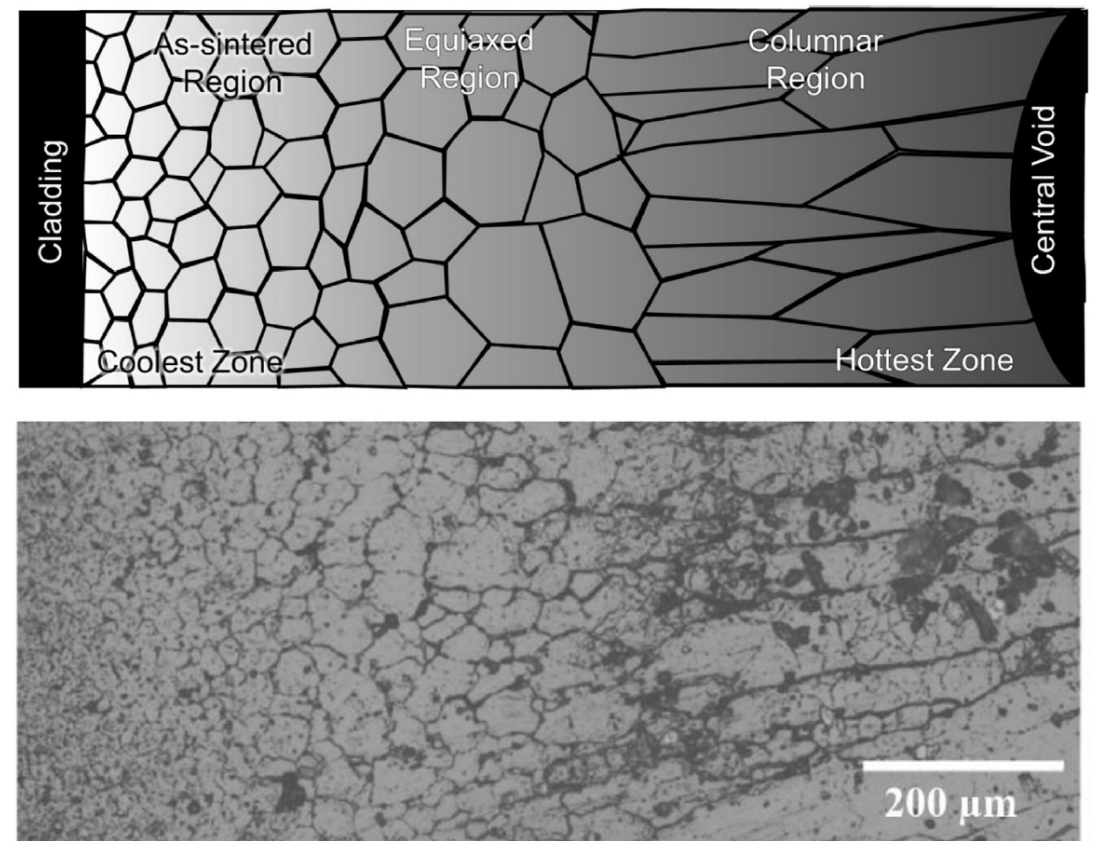
(b)

# MOX Restructuring

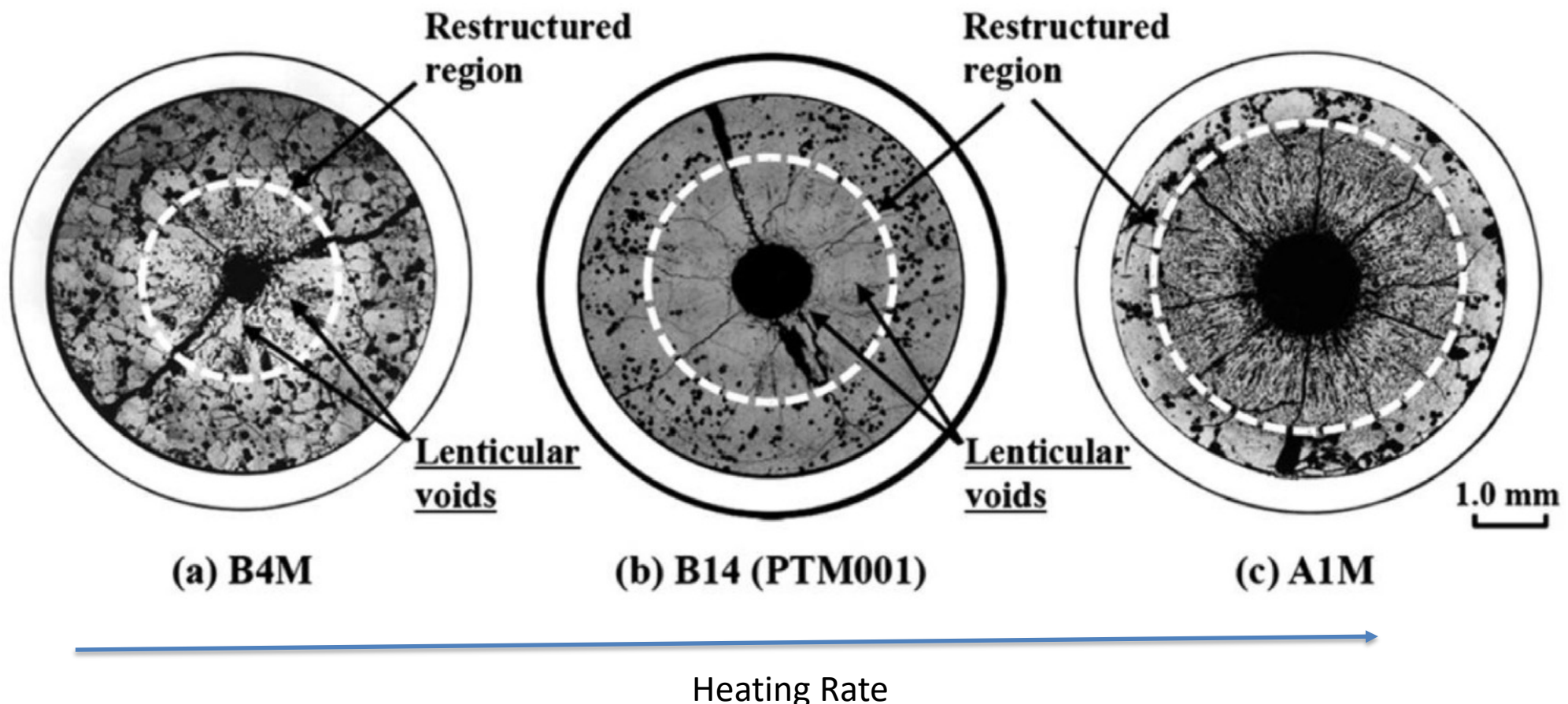
- Oxide nuclear fuels are commonly touted for their outstanding high temperature capabilities under irradiation, but this stability comes the tradeoff of low thermal conductivity
- Due to the low thermal transport, a steep temperature gradient is formed along the radius of the fuel pellet, with the hottest region at the center of the pellet and coolest near the cladding
- This leads to grain growth and restructuring
- Pu bearing fast reactor oxide fuels display four defining regions of a restructured pellet:
  - the central void, the columnar grain growth region, the equiaxed grain growth region, and the as-sintered region
- The higher temperatures and heating rates form coarse, elongated grains that grow radially toward the outer rim of the fuel

# MOX Restructuring

- The equiaxed region consists of grains that have undergone significant growth when compared to the un-irradiated samples
- Central voids have been shown to appear in irradiation times as short as 10 min, demonstrating that the appearance of the central void is a result of fuel temperature and linear heating rate, not high burnup
- The central void forms from the accumulation of voids and pores present in the fuel along a thermal gradient

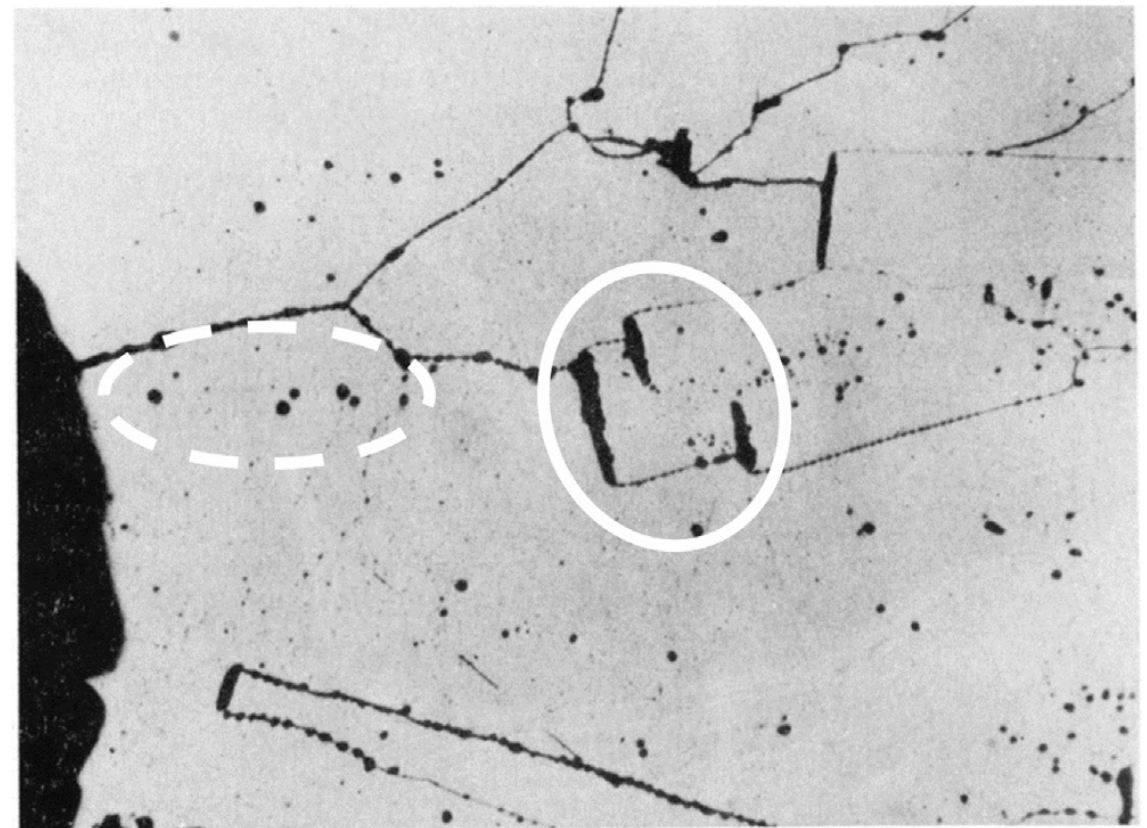


# MOX Pore Formation



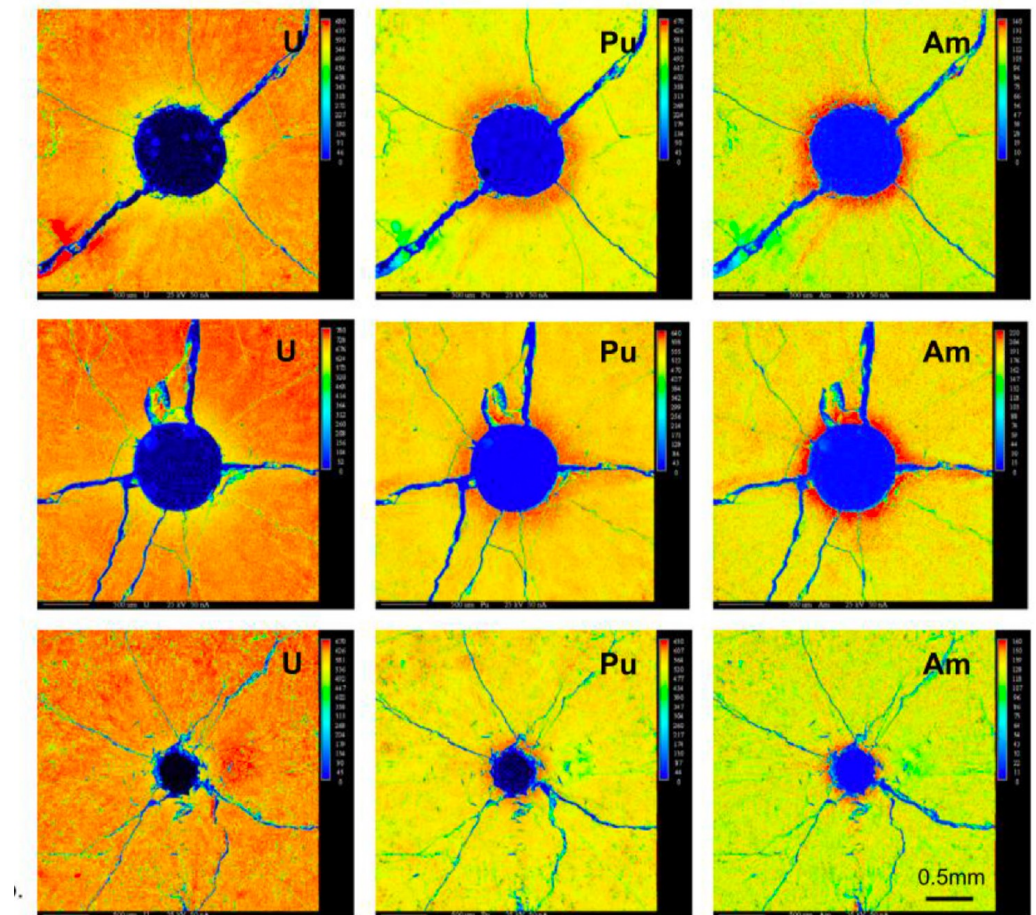
# MOX Pore Formation

- The smallest spherical pores are highly mobile, being able to quickly and easily move through the restructured region
- Intermediate sized pores become flat and elongated as they travel towards the fuel centers, leaving streaks at the tips of the voids as they travel
- These “lenticular” voids are the most readily identifiable porosity feature in the irradiated MOX fuels due to their distinct shape



# Redistribution of Pu

- The movement of pores leads to a redistribution of plutonium, resulting in a spike in Pu concentration surrounding the central void
- Similar behavior has been observed for americium
- This transuranic concentration increase is accompanied with a decrease in U concentration
- This redistribution increases the local fission rate and centerline temperature, while generating lower melting point phases

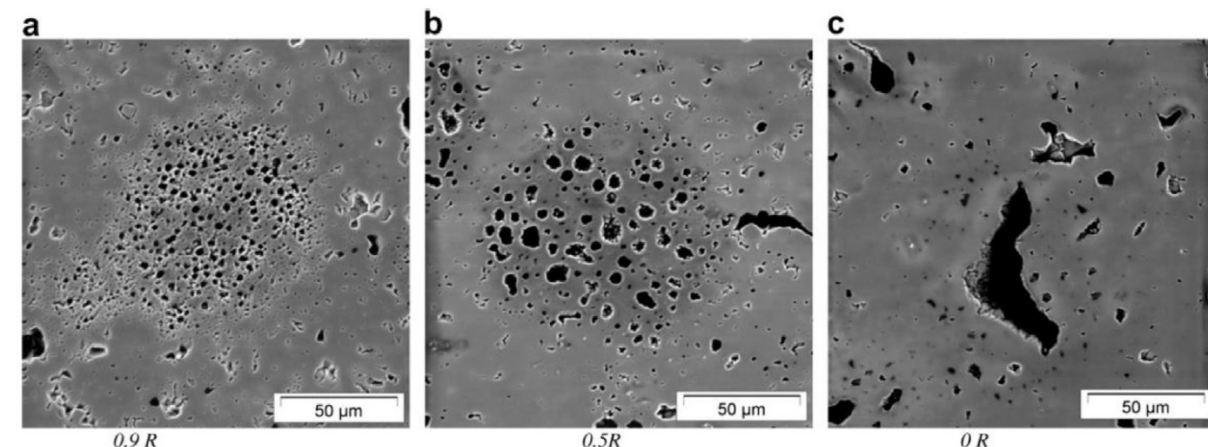


# Redistribution of Pu

- This phenomenon is currently understood as an evaporation-condensation process
- The fuel at the edge of the pore closest to the centerline becomes gaseous inside the pore and deposits itself on the cooler region of the pore closest to the cladding
- UO<sub>2</sub> is the more volatile of the U/Pu heavy metal species present in the fuel matrix
- The high oxygen potential can lead to a high partial pressure of UO<sub>3</sub> within the self-contained pores
- Enriched regions of PuO<sub>2</sub> are left behind and deposited at the leading edge of the central void as the porosity agglomerates in the fuel center
- Some experiments on O/M ratio seems to point towards higher O potential leading to more redistribution
- While this is the working theory, it is not clear if this explanation can also account for the necessary pore velocities
- No experimentally proven substitution has been put forth as a replacement theory to the observed features

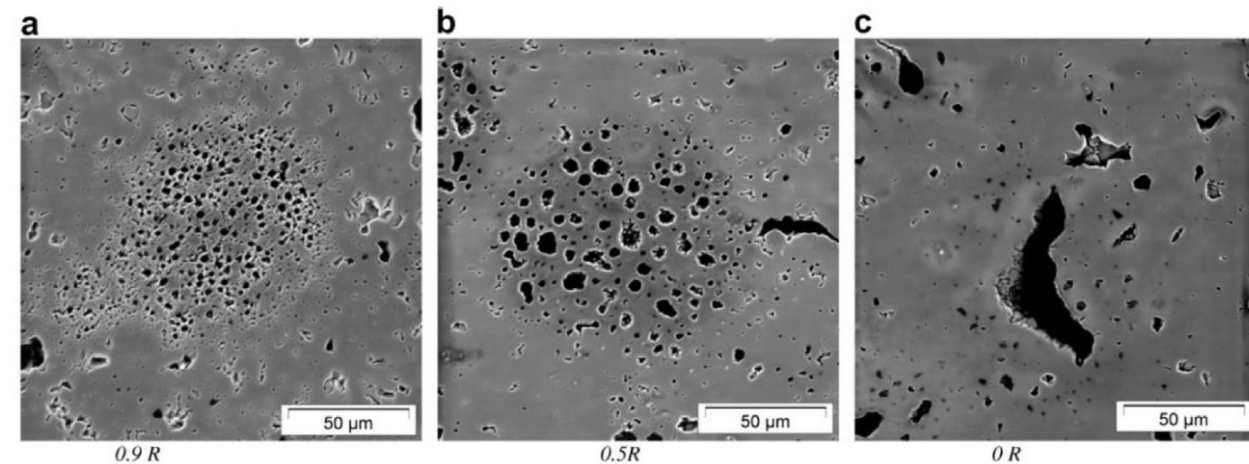
# Pu-rich Agglomerates

- Regions of high Pu concentration form in the MOX fuel matrix due to incomplete mixing during fabrication
- Clusters of dispersed porosity form in the high Pu concentration regions because of the different fission rate
- PA's are highly dense in fissile material, with the high Pu content leading to heating rates and burnups beyond the low concentration UO<sub>2</sub> matrix material
- Thermal conductivity of the spots is also lower than the surrounding matrix, thus the agglomerates are simultaneously hotter and undergo a greater number of fission events in a very small region
- Burnup in these regions may be greater than 2-3 times that of the pellet as a whole



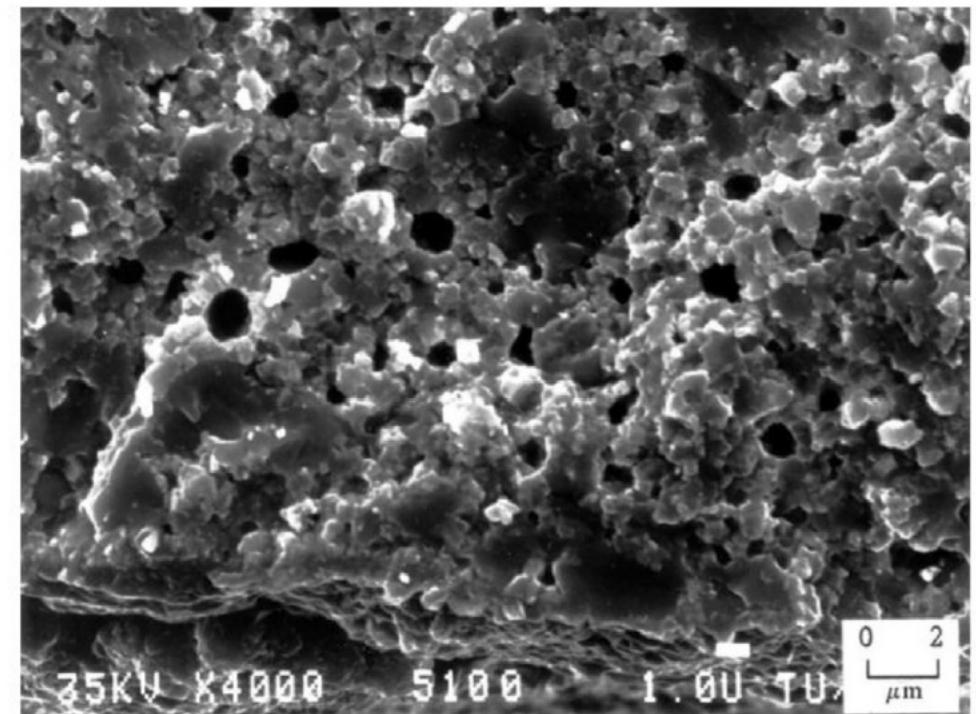
# Pu-rich Agglomerates

- The morphology of porosity in the agglomerates depends on the temperature
- Toward the outer, relatively cool section of the fuel, porosity forms a large number of small bubbles, only 1-2  $\mu\text{m}$  in diameter
- In the intermediate radius of the pellet the densely populated, small pores start to agglomerate to form larger pores
- Near the hot center of the fuel, the bubbles now reach sizes upwards of 50  $\mu\text{m}$  with only a few isolated pores remaining
- Porosity formed due to PA's are visually distinct from those caused by fission gas accumulation on grain boundaries and porosity formed during pellet sintering



# Pu-rich Agglomerates

- The presence of the high burnup structure (HBS) has been observed within the PA regions
- The HBS is basically a fine grained, cauliflower-like structure
- In MOX fuels, the HBS structure appears in fuels following burnups between 60 and 80 GWd/tM at temperatures below approximately 1100C
- PA's reach these local burnups at pellet burnups far below this threshold



# Summary

- Pyroprocessing
  - well established method relying on molten salt and anode deposition
- Metallic fuel performance modeling
  - BISON, ALFUS, LIFEMETAL
  - all still currently require extensive assumptions
- MOX intro
  - restructuring, Pu redistribution, Pu agglomerates

# QUESTIONS?